Scientia Iranica B (2023) 30(2), 376–390

Sharif University of Technology
Scientia Iranica
Transactions B: Mechanical Engineering
http://scientiairanica.sharif.edu

Computational analysis of radiative non-Newtonian Carreau nanofluid flow in a microchannel under the magnetic properties

K. Ramesh[a,1], F. Mebarek-Oudina[b,*], A.I. Ismail[c,d], B.R. Jaiswal[e], A.S. Warke[a], R.K. Lodhi[a], and T. Sharma[f]

a. *Department of Mathematics, Symbiosis Institute of Technology, Symbiosis International University, Pune-412115, India.*
b. *Department of Physics, Faculty of Sciences, University of 20 Août 1955-Skikda, B. P. 26, 21000 Skikda, Algeria.*
c. *Department of Mechanical Engineering, College of Engineering and Islamic Architecture, Umm Al-Qura University, Makkah, Saudi Arabia, P.O. Box 5555 Makkah.*
d. *Department of Mathematics, Faculty of Science, Tanta University, Tanta, P.O. Box 31527, Egypt.*
e. *Department of Mathematics, Symbiosis Institute of Technology, Symbiosis International University, Nagpur-440008, India.*
f. *Department of Mathematics, Lovely Professional University, Jalandhar-144411, India.*

Received 30 June 2021; received in revised form 18 June 2022; accepted 7 November 2022

KEYWORDS
Electroosmotic flow;
Regular perturbation method;
Thermal radiation;
Nanofluid dynamics;
Helmholtz-Smoluchowski velocity;
Slip boundary conditions.

Abstract. Microfluidic technology and Micro Electromechanical Systems (MEMSs) have received much attention in science and engineering fields over the last few years. MEMSs are found in many areas like heat exchangers, chemical separation devices, biochemical analysis, and micro pumps. Keeping these facts in mind, the prime purpose of the current paper is to present the flow of Carreau nanofluids through a microchannel with electro-osmosis, Joule heating, and chemical reactions. The effect of the external magnetic field is considered into account. For the problem formulation, the Cartesian coordinate system is considered. The perturbed solutions are presented by making use of regular perturbation method. The graphical results are prepared based on different values of fluid flow phenomena like velocity, temperature, solutal nano-particle concentration, Sherwood number, and Nusselt number with different fluid variables. According to our analysis, velocity decrement is identified with respect to enhancing the magnetic parameter (Hartmann number). The Schmidt number, Radiation term, Prandtl number, and chemical reaction term increased the solutal nano-particle concentration. The outcomes of the Newtonian liquid model can be obtained from our scrutiny. The present scrutiny has many applications in engineering sciences such as electromagnetic micro pumps and nano-mechanics.

1. Introduction

Over the past few years, the study of nanofluids has attracted continuous consideration because of their various engineering applications. Nanotechnology has become the most important and interesting technology in diverse fields like biology, chemistry, engineering, and physics [1–5]. The technology provides us with plenteous pervasion, which will change the direction

1. *Present address: School of Mathematical Sciences, Sunway University, No. 5, Jalan Universiti, Bandar Sunway, Petaling Jaya 47500, Selangor Darul Ehsan, Malaysia.*
*. *Corresponding author. E-mail address: f.mebarek_oudina@univ-skikda.dz, oudina2003@yahoo.fr (F. Mebarek-Oudina)*

doi: 10.24200/sci.2022.58629.5822

of technological improvements in terms of utilization because of the spread of nanofluids in thermal conductivity, potential advantages, and several applications in biomedical engineering such as cancer treatment using thermal therapy, power generation, heat exchanger, transportation, microelectronics, ventilation, air conditioning, and atomic framework cooling. Nanofluid plays an important role in the functioning of nanotechnology. It also has many industrial applications such as plastic production, expulsion, liquefaction, hot moving, glass fiber creation, wire drawing, and elastic plates. Salahuddin et al. [6] investigated the flow of Carreau nanofluids influenced by a stretching cylinder utilizing Keller box technique with slip effects. Mabood et al. [7] scrutinized the impacts of magnetohydrodynamics and thick dispersal on the laminar boundary layer stream of nanoliquid through a nonlinear extending sheet. Waqas et al. [8] discussed the flow of a Carreau nanoliquid via the exponentially convected stretchable area and this model was evaluated by Range-Kutta-Fehlberg technique. Hatami and Jing [9] presented a differential transformation method to study viscous nanofluid flow. Din et al. [10] explored the impact of mass and heat exchange on the flow of a nanofluid between two plates utilizing homotopy analysis technique. Hayat et al. [11] scrutinized the steady laminar boundary layer flow of a Carreau nanoliquid via a stretching sheet and discussed the impacts of Brownian movement and thermophoresis. Acharya et al. [12] presented the squeezing flow of nanoliquids including Cu-H_2O and Copper-kerosene among two plates using differential transformation technique. Kumar et al. [13] presented heat transfer mechanism and nanofluid microchannel applications using heat convection techniques. Irfan et al. [14] built up a scientific connection for unsteady 3D constrained Carreau nano-liquid convective flow through an extended surface. Rana and Bhargava [15] considered the laminar boundary flow of a nanoliquid via a nonlinear stretching sheet and solved the resulting nonlinear governing equations via variational finite element technique. Rohni et al. [16] contemplated the time-dependent flow through a ceaselessly contracting area with wall mass suction into H_2O-based nanofluids. Sheikholeslami and Ganji [17] investigated the nanofluid stream and heat transfer through the plates at an equi-distance utilizing differential transformation technique. Sheikholeslami et al. [18] introduced the shaky or unsteady flow of a nanofluid squeezing among two plates utilizing adomian decomposition scheme. Sheikholeslami et al. [19] scrutinized the free convection of nanofluids using lattice Boltzmann technique. Ali et al. [20] employed bvp4c MATLAB scheme to investigate the cross nanofluid flow in the process of melting. Shah et al. [21] presented the solutions of Kellor box and bvp4c for the cross nanofluid flow with a chemical process on a melting surface. Ayub et al. [22] used bvp4c solutions to study the radiative 3D cross nano-liquid motion with buoyancy opposing/assisting effects. Haider et al. [23] obtained numerical solutions for the movement of second-grade nanofluid via a stretching surface using bvp4c scheme of MATLAB. Ayub et al. [24] applied bvp4c and Kellor box methods to discuss the cross nanofluid flow in the case of the melting heat transfer in the blood.

In the areas of technology and science, the Magneto-Hydrodynamic (MHD) flow of the non-Newtonian liquids has received much attention. This attention results from many applications in innovation and science, e.g., structure for cooling atomic reactors, blood stream estimation procedures, turbo apparatus development of heat exchangers, establishment of atomic quickening agents, and so on. Internal flows of MHD fluid in ducts and channels have received special attention. Investigators are aware of the fact that the magnetic field has the power to induce current in a progressive conductive liquid and it, in turn, exert force on liquid with varying magnetic fields. This entire basic idea is the supporting pillar of MHD introduction. When an electrically permitting fluid flows through a magnetic field, the interaction between the electromagnetic field and hydrodynamics produces MHDs. Impact of magnetic field on nanofluids with various geometries has been examined by many investigators. Haq et al. [25] presented the stagnation point flow of a nanoliquid with MHDs and thermal radiation effects. Ellahi and Riaz [26] explored the impact of MHDs through the pipe flow of a third-grade liquid with variable viscosity. Ramesh and Sharma [27] presented the fundamental flows of MHD Carreau liquid and introduced slip boundary conditions with radiation parameters and Joule heating utilizing regular perturbation method. The flow and heat transport of MHD Go-H_2O nanofluids among two flat plates was investigated by Dogonchi et al. [28] using Duan-Rach approach in the presence of thermal radiation. Pushpa et al. [29] studied the heat transfer of copper-water nanoliquid in a cylindrical annulus with baffle. Khan et al. [30] presented the MHD squeeze flow of electrically conducting liquid among two parallel disks with suction/injection surface and hybrid nanofluid. Kandasamy et al. [31] examined a nano-particle shape using the pressed MHD nanofluid stream of ethylene glycol, water, and motor oil through a permeable sensor area under thermal radiation. Nadeem and Akbar [32] scrutinized the Peristaltic transfer of Newtonian MHD liquid with variable viscosity in a symmetric channel under the impact of heat transport using adomian decomposition method. Nadeem and Akram [33] investigated the impacts of partial slip over the peristaltic stream of a MHD Newtonian liquid in a non-symmetric channel. Warke et al. [34] presented the MHD flow of micropolar liquid induced by a heated stretching sheet and nonlinear radiation. Srinivas and Kothandapani [35] investigated the impacts of mass and heat transport on peristaltic transfer in a permeable space with consistent walls. Hayat and Hina [36] showed the impacts of mass and heat transport on the MHD peristaltic flow into a planar channel through compliant walls. Some more recent and important studies in the direction of MHD nanoliquid flows in diverse directions can be seen in [37–51] and the references therein.

The Micro Electromechanical System (MEMS) and microfluidic technology enjoy many applications in different branches of engineering and science like lab-on-a-chip system in favor of drug conveyance, heat exchangers, micro pumps, chemical separation devices, biomedical diagnostics, and bio-chemical analysis. Heat transport and fluid flow inside microchannels are involved in all the above-mentioned devices and instruments [52]. One of the significant difficulties in micro-scale transport phenomenon is to have a reliable flow invitation. The most commonly used flow activation mechanism in micro devices involves creating a pressure gradient with a pumping device. Such procedures are cumbersome, utilize moving parts to generate flow, and require frequent upkeep. In the previous decade, utilization of electro-kinetics as a stream impelling system in micro devices is becoming increasingly famous. Given the remotely applied electric field, stream incitation in microchannels has striking applications in various micro-fluidic devices and systems. Keeping all these applications in mind, many researchers have focused their research on microchannel flows with electric fields. Sridhar and Ramesh [53] presented an analytical investigation of the Electro-Magneto-Hydrodynamic (EMHD) radiative Jeffrey nano-liquid flow in an asymmetric peristaltic mechanism. Munawar and Saleem [54] discussed the motion of Williamson hybrid nano-liquid through ciliated walls with EMHD effects. Ijaz et al. [55] provided mathematica solutions for the EMHD nano-bio-fluid flow in a peristaltic curved plate. Mandal et al. [56] discussed the propulsion of superimposed liquids in strait confinements in the presence of EMHD effects. Ghorbani et al. [57] proposed finite-difference solutions for the effect of EMHD on the motion of Carreau-Yasuda liquid through a rectangular microchannel. Murtaza et al. [58] used the Laplace transform technique to discuss the flow of EMHD Maxwell nanofluid in a channel. Noreen et al. [59] discussed the EMHD nanofluid motion through asymmetric peristaltic plates with various zeta potentials. Mahapatra Bandopadhyay [60] analyzed the motion of electro-osmotic viscoelastic liquid over the surfaces of high zeta potentials.

Based on these findings, the present work deals with a novel model for simulating the flow of solar MHD Carreau-nanofluid due to electroosmosis, which can be considered as generalization of the viscous fluid model. The working liquid is a magnetized Carreau nanofluid that includes a base liquid containing suspended magnetic nano-particles. The curiosity of the current work is the consolidation of MHDs and nanofluids dynamics to design a hybrid solar pump system model. The problem is first modeled and then, the perturbation solutions are evaluated for the resulting system of equations. The graphical results are prepared for velocity, solutal nano-particle concentration, temperature, Nusselt number, and Sherwood number. This model facilitates examining the fluid dynamics problems administered by the electroosmosis mechanism. This study is structured as follows: Section 2 describes the modeling of the problem along with the solutions. Section 3 provides numerical outcomes and discussion. Section 4 concludes this study.

2. Modeling

Consider the incompressible flow of a Carreau nanoliquid in the microchannel with distance $2h$. The Cartesian system (x, y) is considered here to study the present problem. In this system, x-axis is in the horizontal direction of fluid movement, while y-axis is taken vertical to it with its origin at the microchannel center. In transverse motion, liquid is conceived to be electrically conducting with an applied magnetic field of magnitude B_0. Fluid particles are confined between two walls. The upper and lower walls have been kept up at steady temperature T_0 and C_0 is the nano-particle volume fraction for these walls. Electroosmotic flow has been taken into consideration and it gives rise to the bulk motion of ionized fluid on a fixed charged surface. The schematic delineation of electroosmotic stream along the horizontal microchannel is depicted in Figure 1. Accordingly, it has been observed that the surface of channel walls is attached with net-negative charges due to which $-ve$ ions get repulsed away from the wall and $+ve$ ions get pulled in towards the wall, shaping an EDL (Electric Double Layer) near the channel wall. At a point where the EDL collaborates with the applied electric field, electroosmotic flow is generated. The $+vely$ charged ions of the EDL layer are magnetized near cathode and repulsed via the anode resulting in net transport of ionized fluid towards the electric field.

The equations of continuity, motion, energy, and solutal-nano-particle concentration for Carreau nanofluids can be incorporated in the following form [27,61]:

$$\nabla \cdot \bar{q} = 0, \tag{1}$$

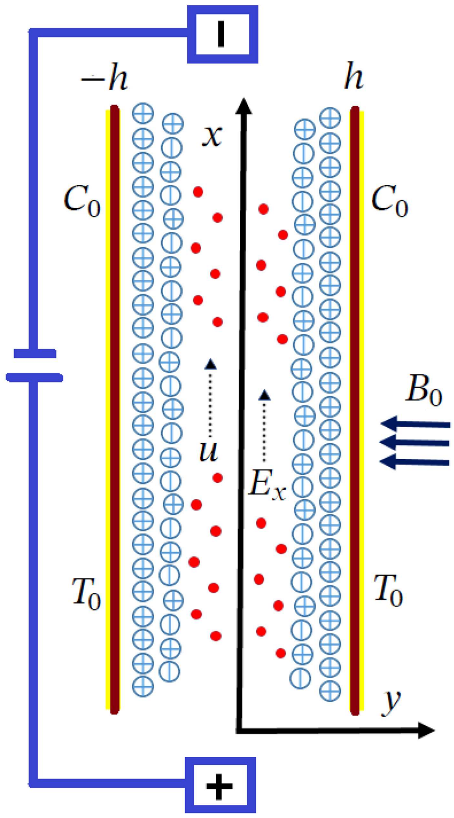

Figure 1. Physical sketch of the electroosmosis-modulated flow of a Carreau nano-liquid in a micro channel.

$$\rho_{ef}\left(\frac{\partial \bar{q}}{\partial t}+(\bar{q}\cdot\nabla\bar{q})\right)=-\nabla P+\nabla\cdot\bar{S}+\bar{J}\times\bar{B}$$

$$+\bar{f}_g+\rho_e E_x, \tag{2}$$

$$(\rho c_p)_{ef}\left(\frac{\partial \bar{q}}{\partial t}+(\bar{q}\cdot\nabla T)\right)=k_{ef}\nabla^2 T+D_{tc}\nabla^2 C$$

$$+\nabla\cdot q_r+\sigma_{ef}E_x^2, \tag{3}$$

$$\frac{\partial C}{\partial t}+(\bar{q}\cdot\nabla C)=D_s\nabla^2 C+D_{ct}\nabla^2 T-k(C-C_0), \tag{4}$$

where the velocity vector is $\bar{q}=(u(y),0,0)$, ρ_{ef} the effective density of nanofluids, P the pressure, $\bar{J}$ the electric current density, $\bar{B}$ the total magnetic field, $\bar{f}_g=\rho_{ef}g(\beta_t(T-T_0)+\beta_c(C-C_0))$, ρ_e electrical charge density, E_x applied electrical field, c_p specific heat at constant pressure, $(\rho c_p)_{ef}$ the heat capacity of the nanofluids, T the temperature, t the time, k_{ef} the effective thermal conductivity, σ_{ef} the electrical conductivity, C the solute concentration, and $\bar{S}$ the extra stress tensor, which is given by [11,27]:

$$\bar{S}=\left\{\left(\eta_\infty+(\eta_0-\eta_\infty)\left(1+\Gamma\bar{\dot{\gamma}}\right)^a\right)^{\frac{w-1}{a}}\right\}\bar{\dot{\gamma}}_{ij}, \tag{5}$$

where:

$$\bar{\dot{\gamma}}=\sqrt{\frac{1}{2}\sum_i\sum_j\bar{\dot{\gamma}}_{ij}\bar{\dot{\gamma}}_{ji}}=\sqrt{\frac{1}{2}}\Pi. \tag{6}$$

Herein, Π stands for the second invariant strain tensor, η_∞ viscosity of fluid at an infinite shear rate, η_0 viscosity of fluid at zero shear rate, Γ and a non-Newtonian liquid quantities, w dimensionless power law index, and $\bar{\dot{\gamma}}$ shear rate. The limiting cases can be captured for shear thickening and shear thinning impacts when $w<1$ and $w>1$, respectively. In the ongoing investigation, $\mu_\infty=0$ is considered. Besides, for $a=2$, this model provides the Carreau fluid model. For $\Gamma=0$ or $w=1$, it is a Newtonian fluid model.

According to the notable Poisson-Boltzmann equation for the microchannel, the electric potential ϕ is defined as follows [61]:

$$\nabla^2\phi=-\frac{\rho_e}{\varepsilon_{ef}}, \tag{7}$$

where $\rho_e=ez(\bar{n}_+-\bar{n}_-)$ represents electrical charge density, $\bar{n}_+$ and $\bar{n}_-$ denote positive and negative ions, respectively, containing bulk concentration, and ε_{ef} is medium permittivity.

Nernst-Planck condition ascertains the potential dispersion and portrays the charge number density for every species as follows:

$$\frac{\partial \bar{n}_\pm}{\partial t}+(\bar{q}\cdot\nabla)\,\bar{n}_\pm=D\nabla^2\bar{n}_\pm\pm\frac{Dze}{k_BT}\left(\nabla\cdot(\bar{n}_\pm\nabla\phi)\right), \tag{8}$$

where D denotes the diffusivity of chemical species. Here, Einstein formula for the species mobility is considered for both of the species with equal ionic diffusion coefficients. It is appropriate to stabilize the conservation equations; in this manner, non-dimensional parameters are introduced as follows:

$$\bar{x}=\frac{x}{h},\quad \bar{y}=\frac{y}{h},\quad \bar{u}=\frac{u}{U},\quad M=\sqrt{\frac{\sigma_{ef}}{\eta_0}}B_0h,$$

$$\bar{T}=\frac{T-T_0}{T_0},\quad \bar{C}=\frac{C-C_0}{C_0},\quad \gamma=\frac{\Gamma U}{h},$$

$$G_{rt}=\frac{\rho_{ef}gh\beta_tT_0}{\eta_0U},\quad G_{rc}=\frac{\rho_{ef}gh\beta_cT_0}{\eta_0U},$$

$$\kappa=hez\sqrt{\frac{2n_0}{\varepsilon_{ef}\kappa_BT_v}},\quad \bar{n}=\frac{n}{n_0},\quad \xi_1=\frac{L_2}{h},$$

$$\xi_2=\frac{L_3}{h},\quad U_{HS}=-\frac{E_x\varepsilon_{ef}\varsigma}{\eta_0U},\quad S=-\frac{\sigma_{ef}E_x^2h^2}{k_{ef}T_0},$$

$$N_{tc}=\frac{D_{tc}C_0}{k_{ef}T_0},\quad N_{ct}=\frac{D_{ct}T_0}{D_sC_0},\quad \beta=\frac{L_1}{h}, \tag{9}$$

here, M is the Hartmann number, u the dimensionless axial component, $\bar{T}$ the non-dimensional temperature, $\bar{p}$ the non-dimensional pressure, $\bar{C}$ the non-dimensional solute nanoparticle concentration, G_{rc} the solutal Grashof number, G_{rt} the thermal Grashof number, n the dimensionless ions bulk concentration in the electrolyte, U_{HS} velocity of the Helmholtz-Smoluchowski, S the Joule heating parameter, N_{tc} the Dufour thermo-diffusive parameter, N_{ct} Soret diffuso-thermo parameter, and ϕ dimensionless electric potential term. In a steady state, the Poisson-Boltzmann condition is reduced to the following:

$$\frac{d^2\phi}{dy^2} = -\kappa^2\left(\frac{n_+ - n_-}{2}\right), \tag{10}$$

where κ stands for the electroosmotic term. The ionic dissemination can be achieved using Nernst Planck equation, which is defined as:

$$\frac{d^2 n_\pm}{dy^2} \pm \frac{d}{dy}\left(n_\pm \frac{d\phi}{dy}\right) = 0, \tag{11}$$

exposed to the conditions featuring $\phi = 0$, $n_\pm = 1$, and $\frac{\partial n_\pm}{\partial y} = 0$ at $\frac{\partial \phi}{\partial t} = 0$. In this condition, a much-anticipated Boltzmann dispersion for the ions is obtained as follows:

$$n_\pm = e^{\mp\phi}. \tag{12}$$

By substituting Eq. (12) in Eq. (10), the Poisson-Boltzmann model for the electrical potential dissemination in the electrolyte is obtained and it yields the following:

$$\frac{d^2\phi}{dy^2} = \kappa^2 \sinh(\phi). \tag{13}$$

Further, based on the estimate of low-zeta potential, Eq. (13) is linearized, which tends to be disentangled as:

$$\frac{d^2\phi}{dy^2} = \kappa^2 \phi. \tag{14}$$

Eq. (14) can be simplified under the conditions $\left.\frac{\partial\phi}{\partial t}\right|_{y=0} = 0$ and $\phi|_{y=1} = 1$, whereas the potential function solution can be composed as:

$$\phi = \frac{\cosh(\kappa y)}{\cosh\kappa}. \tag{15}$$

Using the above-mentioned assumptions along with the dimensionless quantities, the subsequent governing differential equations (after dropping the bars) can be composed as:

$$\frac{d^2u}{dy^2} + \frac{3}{2}(w-1)\gamma^2\left(\frac{du}{dy}\right)^2\left(\frac{d^2u}{dy^2}\right) - M^2u + \kappa^2 U_{HS}\frac{\cosh(\kappa y)}{\cosh\kappa} + G_{rt}T + G_{rc}C = 0, \tag{16}$$

$$(1 + RnPr)\frac{d^2T}{dy^2} + N_{tc}\frac{d^2C}{dy^2} + S = 0, \tag{17}$$

$$\frac{d^2C}{dy^2} + N_{tc}\frac{d^2T}{dy^2} - \alpha ScC = 0, \tag{18}$$

with the non-dimensional form of slip boundary condition being as follows:

$$u - \beta\left(\frac{du}{dy} + \frac{1}{2}(w-1)\gamma^2\left(\frac{du}{dy}\right)^3\right) = U_1,$$

$$T - \xi_1\frac{dT}{dy} = 0, \qquad C - \xi_2\frac{dC}{dy} = 0 \qquad \text{at} \quad y = -1, \tag{19}$$

$$u + \beta\left(\frac{du}{dy} + \frac{1}{2}(w-1)\gamma^2\left(\frac{du}{dy}\right)^3\right) = U_2,$$

$$T + \xi_1\frac{dT}{dy} = 0, \qquad C + \xi_2\frac{dC}{dy} = 0 \qquad \text{at} \quad y = 1. \tag{20}$$

In general, ($U_1 = 0$ and $U_2 = 0$) are considered. However, the current findings are extended to diverse values of U_1 and U_2 graphically (meaning that the upper and lower plates are moving in different directions with constant velocities). Using Eqs. (16)–(18) with the assistance of boundary Conditions (19) and (20), the expressions for solutal nano-particle concentration, temperature, and velocity distributions are obtained as follows:

$$C = C_1 e^{my} + C_2 e^{-my} - \frac{R}{m^2}, \tag{21}$$

$$T = B_1 e^{my} + B_2 e^{-my} + B_3 y^2 + C_3 y + C_4, \tag{22}$$

$$\begin{aligned} u =& C_5 e^{My} + C_6 e^{-My} + B_4(e^{\kappa y} + e^{-\kappa y}) + B_5 e^{my} \\ &+ B_6 e^{-my} + B_7 y^2 + B_8 y + B_9 + \gamma^2(C_7 e^{My} \\ &+ C_8 e^{-My}(B_{10} e^{3My} + B_{11} e^{-3My} + B_{12} e^{3my} \\ &+ B_{13} e^{-3my} + B_{14} e^{3\kappa y} + B_{15} e^{-3\kappa y} + B_{16} e^{2My} \\ &+ B_{17} e^{-2My} + B_{18} e^{2my} + B_{19} e^{-2my} + B_{20} e^{2\kappa y} \\ &+ B_{21} e^{-2\kappa y} + B_{22} e^{my} + B_{23} e^{-my} + B_{24} e^{\kappa y} \\ &+ B_{25} e^{-\kappa y} + B_{26} e^{My} + B_{27} e^{-My} + B_{28} e^{(2\kappa+M)y} \\ &+ B_{29} e^{-(2\kappa+M)y} + B_{30} e^{(M-2\kappa)y} + B_{31} e^{(2\kappa-M)y} \\ &+ B_{32} e^{(2m+M)y} + B_{33} e^{-(2m+M)y} + B_{34} e^{(M-2m)y} \\ &+ B_{35} e^{(2m-M)y} + B_{36} e^{(\kappa+2M)y} + B_{37} e^{-(\kappa+2M)y} \\ &+ B_{38} e^{(\kappa-2M)y} + B_{39} e^{(2M-\kappa)y} + B_{40} e^{(2m+\kappa)y} \end{aligned}$$

$$+ B_{41}e^{-(2m+\kappa)y} + B_{42}e^{(\kappa-2m)y} + B_{43}e^{(2m-\kappa)y}$$
$$+B_{44}e^{(m+2M)y}+B_{45}e^{-(m+2M)y}+B_{46}e^{(2M-m)y}$$
$$+ B_{47}e^{(m-2M)y} + B_{48}e^{(2\kappa+m)y} + B_{49}e^{-(2\kappa+m)y}$$
$$+ B_{50}e^{(m-2\kappa)y} + B_{51}e^{(2\kappa-m)y} + B_{52}e^{(\kappa+M)y}$$
$$+ B_{53}e^{-(\kappa+M)y} + B_{54}e^{(M-\kappa)y} + B_{55}e^{(\kappa-M)y}$$
$$+ B_{56}e^{(m+M)y} + B_{57}e^{-(m+M)y} + B_{58}e^{(M-m)y}$$
$$+ B_{59}e^{(m-M)y} + B_{60}e^{(m+\kappa)y} + B_{61}e^{-(m+\kappa)y}$$
$$+ B_{62}e^{(\kappa-m)y} + B_{63}e^{(m-\kappa)y} + B_{64}e^{(m+\kappa+M)y}$$
$$+ B_{65}e^{-(m+\kappa+M)y} + B_{66}e^{(m-\kappa+M)y}$$
$$+ B_{67}e^{(\kappa-m-M)y} + B_{68}e^{(m+\kappa-M)y}$$
$$+ B_{69}e^{(M-m-\kappa)y} + B_{70}e^{(m-\kappa-M)y}$$
$$+ B_{71}e^{(M+\kappa-m)y} + B_{72}y^2 + B_{73}y + B_{74})), \quad (23)$$

where C_i's $(i = 1, 2, \cdots, 8)$ and B_j's $(j = 1, 2, \cdots, 74)$ are basic algebraic calculations conducted by Mathematica programming software.

3. Results and conversation

Here, the effects of numerous physical parameters through the temperature T, velocity U, solutal nanoparticle concentration C, Sherwood number Sh, and Nu have been considered. According to these figures, velocity, temperature, and solute NPs concentration profiles are almost parabolic in nature.

Figure 2(a) presents the alteration of chemical reaction termαvia velocity dissemination. It is seen that the velocity is reduced upon enhancing the estimations of chemical reaction parameter when Joule heating parameter is positive. This is because the chemical reaction in this system leads to the use of the chemical; hence, velocity declines. However, without Joule heating parameter and with negative values, the velocity increases as the value of chemical reaction parameter increases. Figure 2(b) visualizes the velocity dissemination at different values of β. The increase in velocity followed by the rising values of velocity slip term in all instances of Joule heating parameter is observed in Figure 2(b). It is physically reasonable that while the slipping of liquid takes place at the boundary, liquid velocity is not equivalent to the boundary at that point. Also, since more liquid slips at the boundary, its velocity declines and is influenced by the boundary movement. From Figure 2(c), the velocity declines upon enhancing the estimation of M in every case of the three referenced Joule heating parameters. This is due to the Lorentz force generated via the application of constant magnetic field, which exhibits resistance to the fluid motion and constrains the flow. Figure 2(d) tends to visualize the velocity dissemination at different values of electroosmosis term κ in three different situations of Joule heating parameters. According to Figure 2(d), the velocity increments upon increasing the estimation of electroosmosis parameter. Figure 2(e) presents the behavior of motion of the superior plate via velocity distribution. Increase in velocity in all the cases is observed. For example, in case of the movement of the upper plate to the opposite direction of the flow, both plates are fixed and the top plate moves with a constant velocity. In all these cases, it is additionally noticed that higher velocities are detected due to the movement of the upper plate with a constant velocity. It is concluded that when the plate moves, the layers that are close to the plate are affected, hence higher velocity. Similar results are expected due to the movement of the lower plate (see Figure 2(f)).

Figure 3(a) analyzes the effect of variations in α on the temperature dissemination. It is found that the temperature diminishes with an increase in α when Joule heating term is positive, and the temperature increases when the Joule heating parameter is negative. Figure 3(b) illustrates the variation of Soret diffuso-thermo parameter with respect to the temperature and from this figure, the temperature is enhanced by boosting the estimations of Soret diffuso-thermo term on account of positive estimation of Joule heating term, whereas in the event of negative estimation of Joule heating term, the pattern is reversed. Figure 3(c) shows the effect of variations of Pr on the temperature profile. According to this plot, following the increase in the estimated value of Pr, the temperature for negative Joule heating term increases and the pattern is inverted due to positive Joule heating term. The rise in Prandtl number makes thermal diffusivity more fragile and the thickness of the boundary layer more slender. A larger Prandtl number would have lower thermal diffusivity and lower Pr has higher thermal diffusivity. At a lower value of Pr, the higher temperature dissemination is noticed. A similar behavior is observed in Figure 3(d) and (e) upon enhancing Rn and Sc. In this respect, an increment in Rn reduces the thickness of the boundary layer and increases the rate of heat transport in a dissolving area in the presence of chemical impact. Plot 3(f) depicts the nature of temperature slip term. It is seen that the temperature increments with an increase in the value of the temperature slip parameter when the Joule heating parameter is positive, while the temperature decreases when the Joule heating parameter is negative.

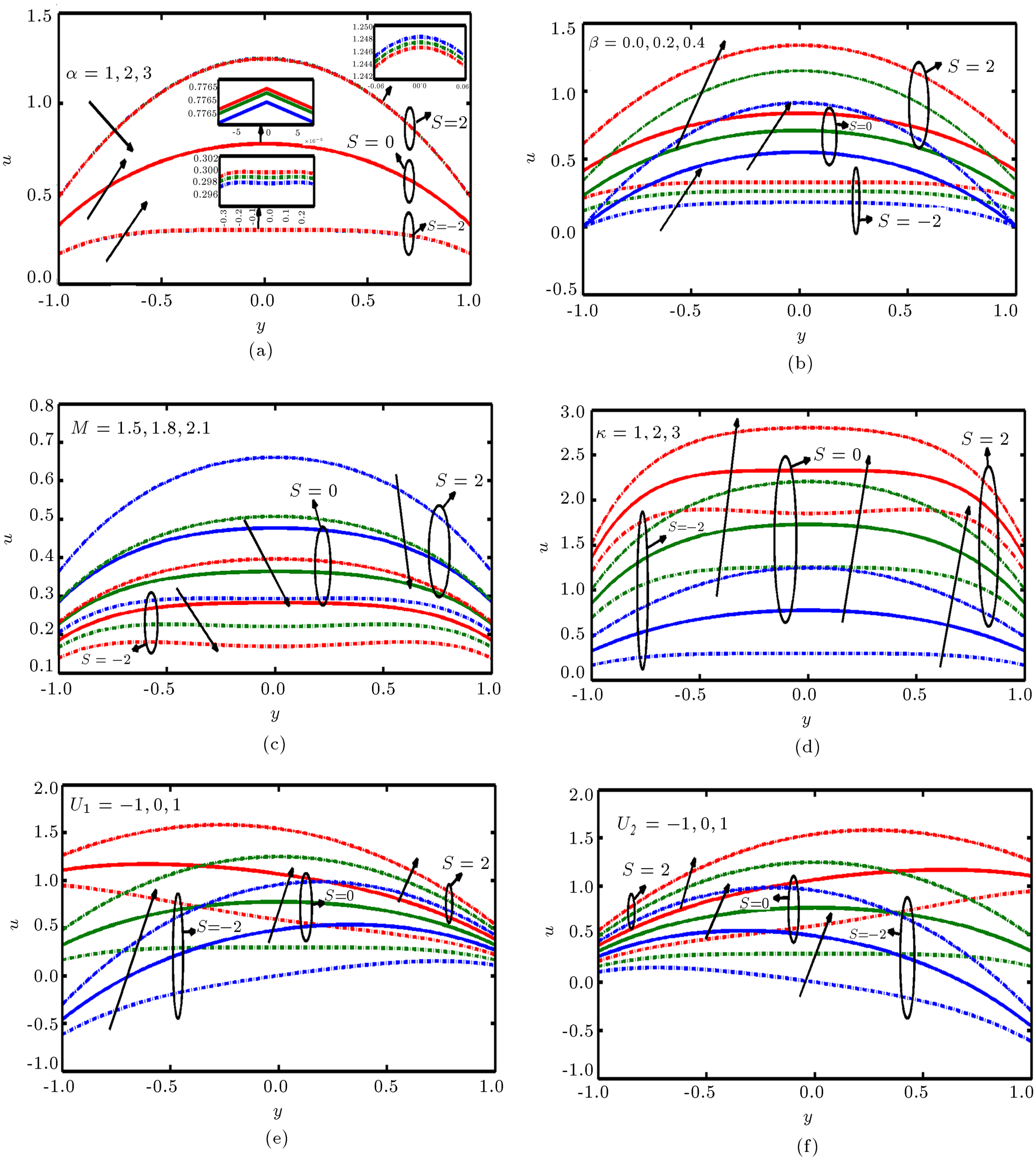

Figure 2. Profiles of velocity for the different fluid parameters.

Figure 4(a) shows the impact of α over the solutal nanoparticle concentration. From this figure, the solutal nanoparticle concentration is a decreasing function of α for negative estimation of Joule warming parameter because the chemical reaction justifies the utilization of the chemical species; therefore, the concentration profile diminishes along the ascending function for positive estimation of Joule heating parameter. Figure 4(b) depicts that with the rise of N_{tc}, the solutal nanoparticle concentration profile keeps increasing for the negative Joule heating term and decreasing for positive Joule heating term. Figure 4(c) shows the fluctuation of different values of Pr in the solutal nanoparticle concentration distribution. Based on Figure 4(c), the rise of Pr leads to the reduction of the solutal nanoparticle concentration profile for $S = -2$ and when $S = 2$, the trend is opposite. Figure 4(d) plots the variations of Rn via the solutal nanoparticle concentration distribution. It is noted that when Joule heating parameter is positive, the solutal-nano-particle concentration is enhanced with an increase in the value of radiation parameter and when Joule heating parameter is negative, the solutal nanoparticle concentration diminishes with increase in the value of radiation parameter. A similar behavior is followed by an increase in Schmidt number Sc (see Figure 4(e)). Increase in the estimate of Sc corresponds to the high rate of viscous dissemination, which causes

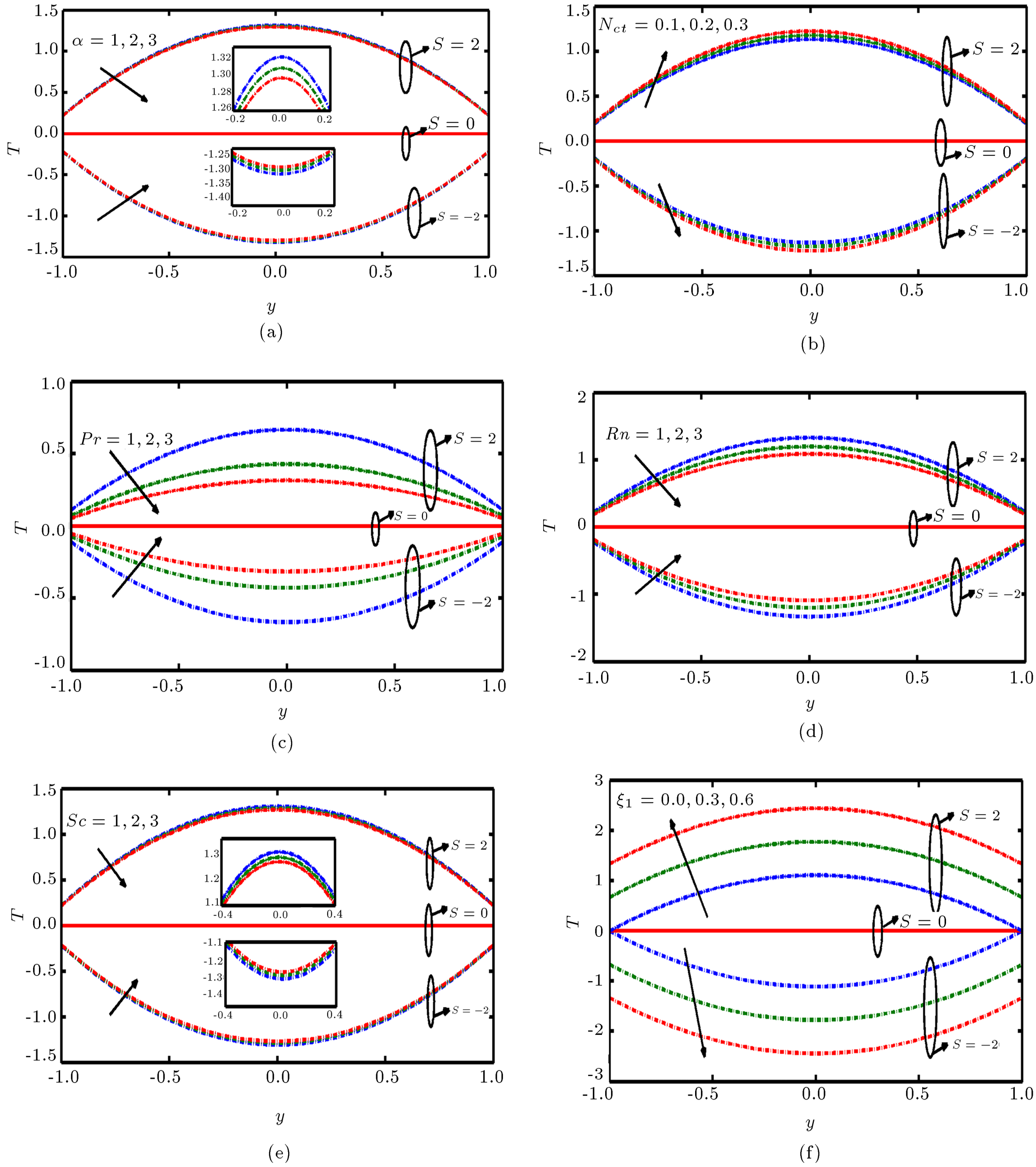

Figure 3. Temperature distributions by the different fluid terms.

an increment in the solutal nano-particle concentration of a fluid. The impact of concentration slip parameter through the solutal NP concentration is described in Figure 4(f). It is obvious from this figure that the concentration augments upon enhancing the value of concentration slip parameter at a negative value of Joule heating term and the pattern is overturned at a positive value of Joule heating term. In all the cases, no variation is noticed for $S = 0$.

Figure 5(a)–(e) visualizes the features between radiation parameter Rn and Nusselt number Nu. From Figure 5(a)–(c), Nu augments with a rise in the values of α, Pr, and Sc at negative values of Joule heating term, while the opposite pattern is pursued at the positive Joule heating term. This is because the development of the radiation term Rn causes a decline in the thickness of the boundary layer and increase in the heat transport rate in the melting area in the presence of chemical impact. Figure 5(d)–(e) plots the impacts of N_{ct} and N_{tc} on Nu. It is noticed that Nu diminishes upon boosting values of N_{ct} and N_{tc} for $S = -2$ and the case is inverted for $S = 2$. To study the effects between radiation term Rn and Sherwood number Sh, Figure 6(a)–(e) has been prepared. According to Figure 6(a)–(c), with an increase in the values of α, Prandtl number, and Sc, there is an increase in

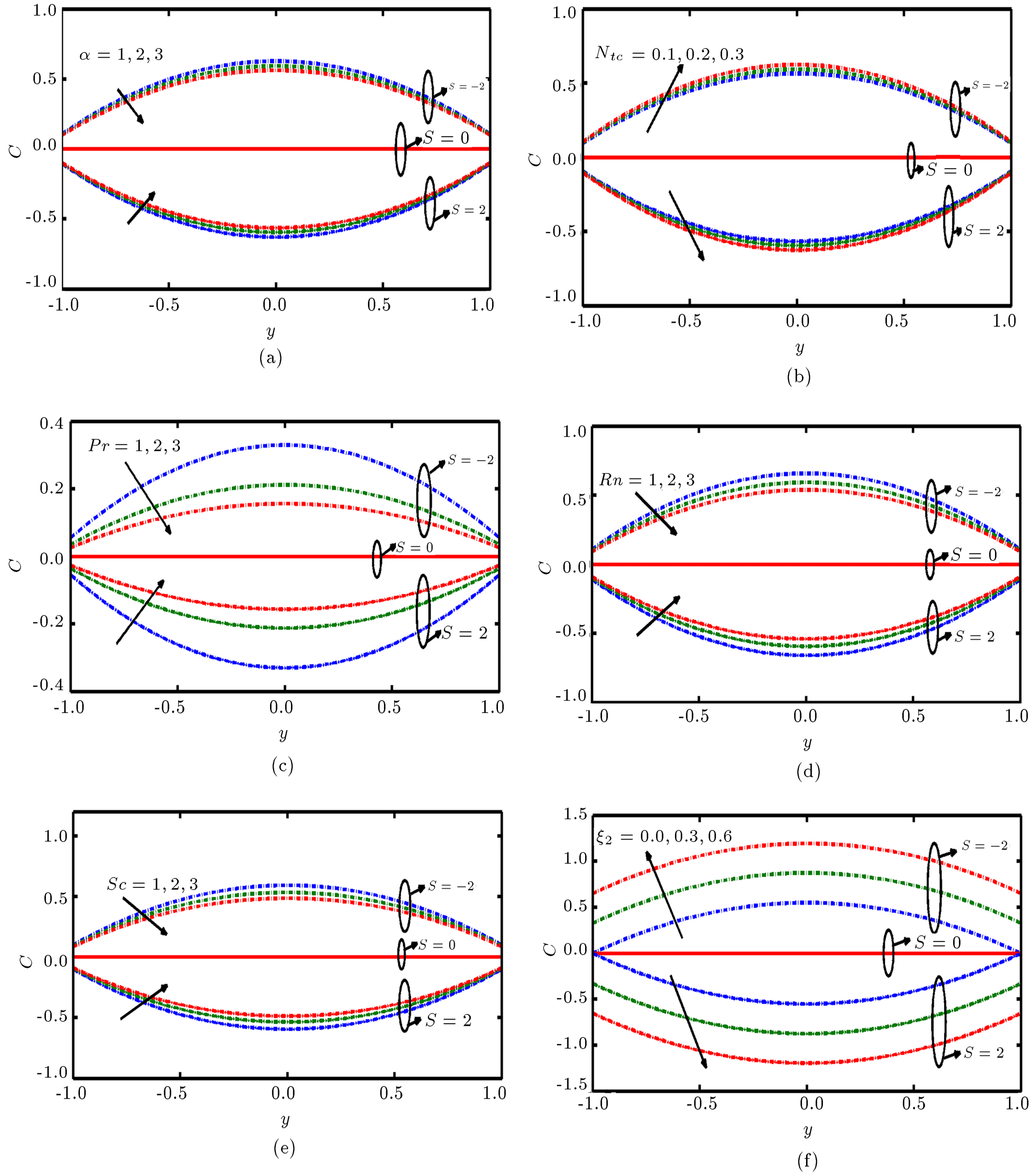

Figure 4. Solutal nanoparticle concentration by the different liquid parameters.

Sherwood number for the non-negative Joule heating term, while the pattern is reversed for the non-positive Joule heating term. Figure 6(d)–(e) visualizes the conduct of N_{ct} and N_{tc} on *Sh*. It is depicted that *Sh* rises upon increasing values of N_{ct} and N_{tc} at a negative value of Joule heating term and Sherwood number is reduced at a positive value of Joule heating term. Without Joule heating term, no change in *Nu* and *Sh* is detected. It is clearly mentioned from Figure 7 that the reported outcomes are in close agreement with the existing results obtained by Ramesh and Sharma [27] in the limiting cases of the current analysis.

4. Conclusions

The current study is a worthwhile attempt to study the transport of Carreau nanofluid in the infinite parallel microchannels. The impacts of radiation, magnetic field, chemical reaction, and Helmholtz-Smoluchowski velocity were considered. The solutions for the temperature, velocity, and solutal nanoparticle concentration were introduced utilizing regular perturbation technique considering Carreau liquid parameter as perturbation parameter. The numerical simulation was presented to illustrate the nature of the flow quantities.

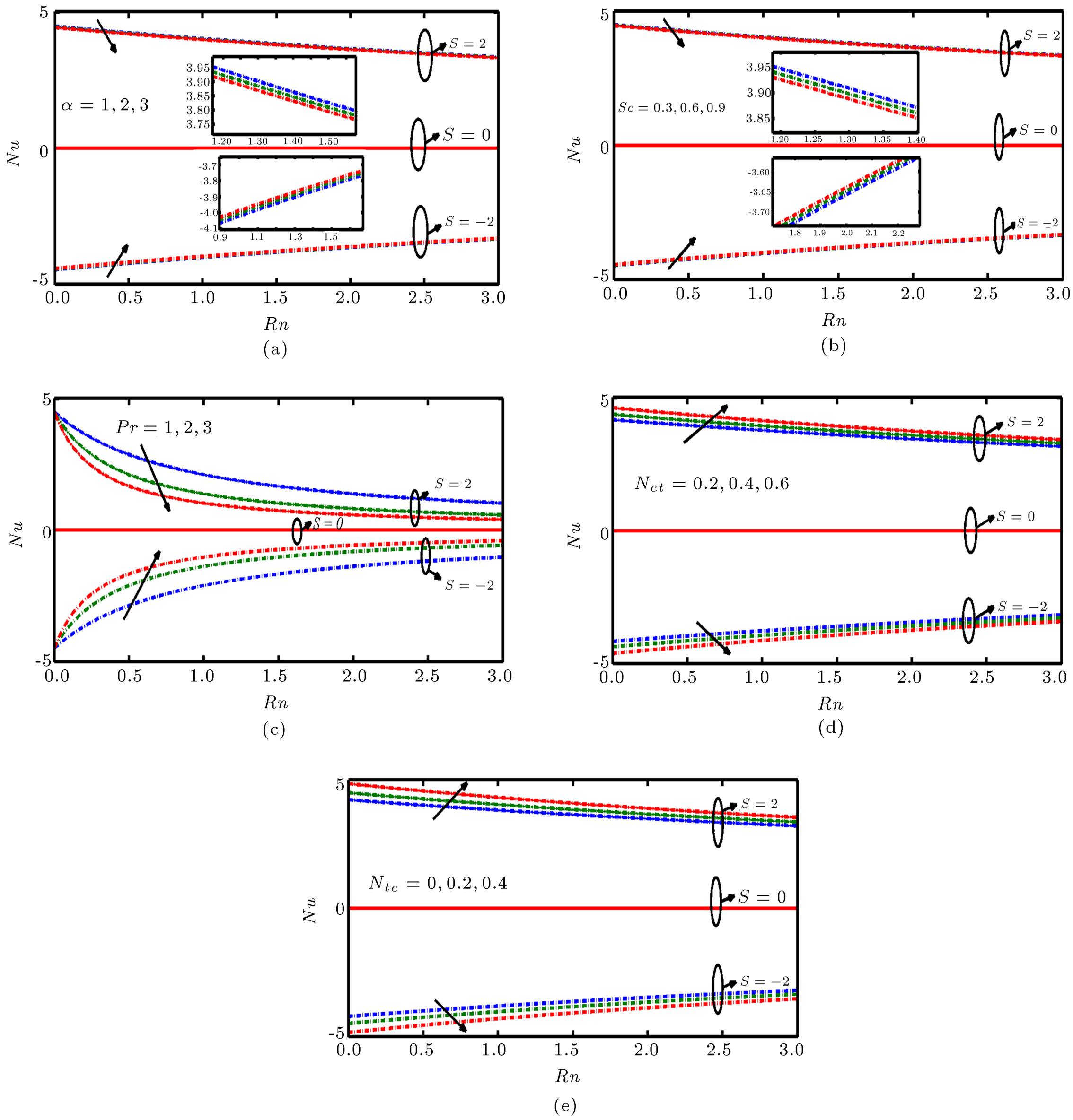

Figure 5. Nu distributions by the different fluid terms.

The obtained findings are summed up in the following form:

- The velocity exhibited a rising function of chemical reaction term and slip velocity parameter in case of negative Joule heating term, while the opposite pattern was seen for positive Joule heating term;
- The velocity declined following the enhancement of Hartmann number in all the cases of Joule heating term;
- The temperature diminished with an increment in α, Pr, Rn, Sc with positive Joule heating term;
- The solutal nano-particle concentration increased via an increment in α, Pr, Rn, and Sc for the positive Joule heating term;
- Very similar observations were obtained in Nu and Sh through all the cases of Joule heating parameter;
- The results of the Newtonian liquid model could be obtained by setting $\gamma = 0$ and $w = 1$.

The findings of the current mathematical scrutiny will be the benchmark for simulating a more generalized model in three dimensions for the nanofluid/hybrid nanofluid flow in different directions with thermophysical properties.

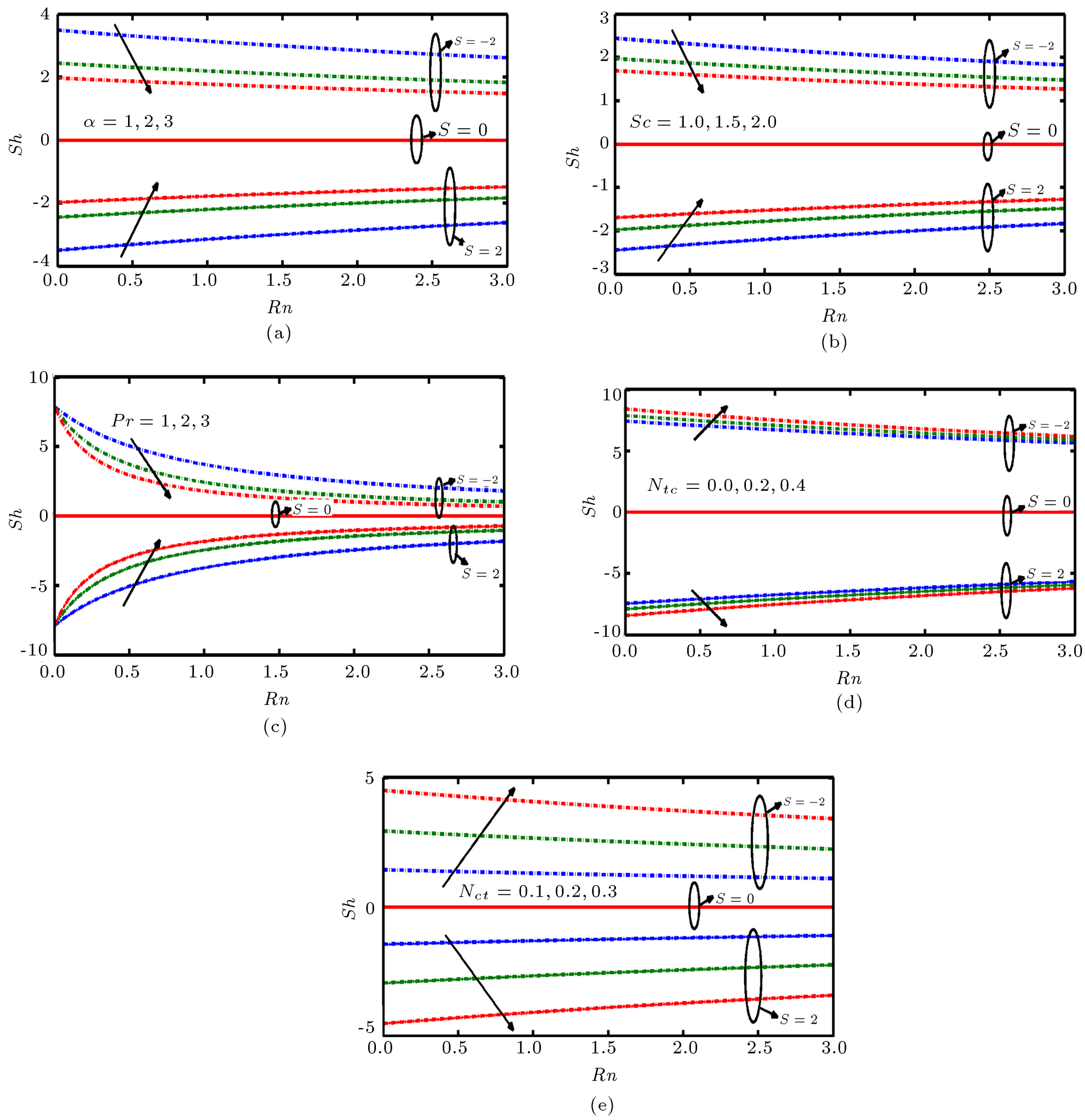

Figure 6. *Sh* distributions for the different fluid parameters.

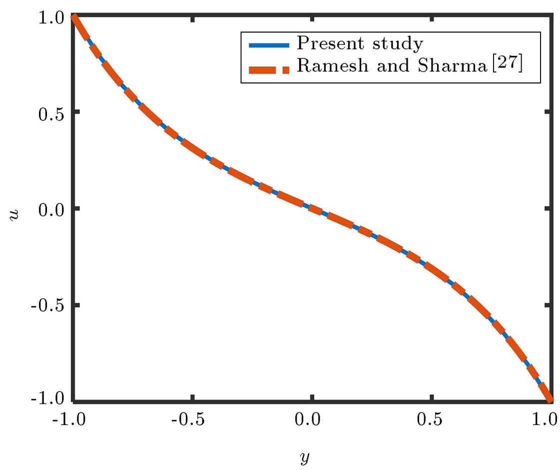

Figure 7. Comparison between velocity profile the existing profile in the literature.

Acknowledgments

The authors would like to thank the Deanship of Scientific Research at Umm Al-Qura University for supporting this work via Grant Code: (22UQU4240002DSR09).

Nomenclature

B_0	Magnetic field strength (T)
x	Axial direction of flow (m)
y	Transverse direction of flow (m)
$\bar{q}$	Velocity vector (m s^{-1})
ρ_{nf}	Effective density of nanoliquid (kg m^{-3})
P	Pressure (Pa)

σ_{ef}	Effective electrical conductivity (S m^{-1})
$(c_p)_{ef}$	Effective heat capacity of the nanofluid (J kg^{-1} K^{-1})
t	Time (s)
k_{ef}	Effective thermal conductivity (W $m^{-1}K^{-1}$)
T	Temperature (K)
C	Concentration of the liquid (mol m^{-3})
D_{tc}	Temperature diffusivity coefficient (m^2 s^{-1})
D_{ct}	Mass diffusivity coefficient (m^2 s^{-1})
E_x	Applied electrical field (V m^{-1})
D_s	Solutal diffusivity (m^2 s^{-1})
k	Chemical reaction parameter (mol m^{-2} s^{-1})
T_0	Ambient temperature (–)
C_0	Ambient concentration (–)
u	Velocity component (m s^{-1})
g	Acceleration due to gravity (m s^{-2})
β_c	Concentration expansion coefficient (K^{-1})
β_t	Thermal expansion coefficient (K^{-1})
η_∞	Viscosity of liquid at infinite shear rate (kg m^{-1} s^{-1})
η_0	Viscosity of liquid at zero shear rate (kg m^{-1} s^{-1})
Γ	Material constant (–)
a	Non-Newtonian liquid constant (–)
ϕ	Electric potential term (V)
ρ_e	Electrical charge density (C m^{-3})
w	Power law index (–)
ε_{ef}	Medium permittivity (F m^{-1})
n	Ions bulk concentration in the electrolyte (m^{-3})
M	Hartmann number (–)
κ	Electro osmosis term (–)
U_{HS}	Helmholtz-Smoluchowski velocity (m s^{-1})
G_{rt}	Thermal Grashof number (–)
G_{rc}	Solutal Grashof number (–)
Pr	Prandtl number (–)
Rn	Radiation parameter (–)
q_r	Radiative heat flux (W m^{-2})
S	Joule heating parameter (–)
N_{tc}	Dufour thermo-diffusive parameter (–)
N_{ct}	Soret diffusion-thermo parameter (–)
α	Dimensionless chemical reaction term (–)
Sc	Schmidt number (–)
ξ_1	Temperature slip term (–)
ξ_2	Concentration slip term (–)
β	Velocity slip parameter (–)
Sh	Sherwood number (–)
Nu	Nusselt number (–)

References

1. Jabeen, S., Hayat, T., and Alsaedi, A. "Entropy generation optimization and activation energy in flow of Walters-B nanomaterial", *Sci. Iran.*, **28**(3), pp. 1917–1925 (2021).
2. Atif, S.M., Hussain, S., and Sagheer, M. "Effect of thermal radiation on MHD micropolar Carreau nanofluid with viscous dissipation, Joule heating, and internal heating", *Sci. Iran.*, **26**(6), pp. 3875–3888 (2019).
3. Shafiq, A., Mebarek-Oudina, F., Sindhu, T.N., et al. "Sensitivity analysis for Walters' B nanoliquid flow over a radiative Riga surface by RSM", *Sci. Iran.*, **29**(3), pp. 1236–1249 (2022). https://dx.doi.org/10.24200/sci.2021.58293.5662.
4. Mebarek-Oudina, F. "Convective heat transfer of Titania nanofluids of different base fluids in cylindrical annulus with discrete heat source", *Heat Transf.-Asian Res.*, **48**(4), pp. 135–147 (2019).
5. Reddy, Y.D., Mebarek-Oudina, F., Goud, B.S., et al. "Radiation, velocity and thermal slips effect toward MHD boundary layer flow through heat and mass transport of Williamson nanofluid with porous medium", *Arabian Journal for Science and Engineering*, **47**(12), pp. 16355–16369 (2022). https://doi.org/10.1007/s13369-022-06825-2
6. Salahuddin, T., Hussain, A., Malik, M.Y., et al. "Carreau nanofluid impinging over a stretching cylinder with generalized slip effects: Using finite difference scheme", *Results Phys.*, **7**, pp. 3090–3099 (2017).
7. Mabood, F., Khan, W.A., and Ismail, A.I.M. "MHD boundary layer flow and heat transfer of nanofluids over a nonlinear stretching sheet: A numerical study", *J. Magn. Magn. Mater.*, **374**, pp. 569–576 (2015).
8. Waqas, M., Khan, M.I., Hayat, T., et al. "Numerical simulation for magneto Carreau nanofluid model with thermal radiation: A revised model", *Comput. Methods Appl. Mech. Eng.*, **324**, pp. 640–653 (2017).
9. Hatami, M. and Jing, D. "Differential transformation method for Newtonian and non-Newtonian nanofluids flow analysis: Compared to numerical solution", *Alex. Eng. J.*, **55**, pp. 731–739 (2016).

10. Din, S.T.M., Zaidi, Z.A., Khan, U., et al. "On heat and mass transfer analysis for the flow of a nanofluid between rotating parallel plates", *Aerosp. Sci. Technol.*, **46**, pp. 514–522 (2015).

11. Hayat, T., Waqas, M., Shehzad, A., et al. "Stretched flow of Carreau nanofluid with convective boundary condition", *Pramana*, **86**, pp. 3–17 (2016).

12. Acharya, N., Das, K., and Kundu, P.K. "The squeezing flow of Cu-water and Cu-kerosene nanofluids between two parallel plates", *Alex. Eng. J.*, **55**, pp. 1177–1186 (2016).

13. Kumar, N., Singh, P., Redhewa, A.K., et al. "A review on nanofluids applications for heat transfer in microchannels", *Procedia Eng.*, **127**, pp. 1197–1202 (2015).

14. Irfan, M., Khan, M., and Khan, W.A. "Numerical analysis of unsteady 3D flow of Carreau nanofluid with variable thermal conductivity and heat source/sink", *Results Phys.*, **7**, pp. 3315–3324 (2017).

15. Rana, P. and Bhargava, R. "Flow and heat transfer of a nanofluid over a nonlinearly stretching sheet: A numerical study", *Commun. Nonlinear Sci. Numer. Simul.*, **17**, pp. 212–226 (2012).

16. Rohni, A.M., Ahmad, S., and Pop, I. "Flow and heat transfer over an unsteady shrinking sheet with suction in nanofluids", *Int. J. Heat Mass Transf.*, **55**, pp. 1888–1895 (2012).

17. Sheikholeslami, M. and Ganji, D.D. "Nanofluid flow and heat transfer between parallel plates considering Brownian motion using DTM", *Comput. Methods Appl. Mech. Eng.*, **283**, pp. 651–663 (2015).

18. Sheikholeslami, M., Ganji, D.D., and Ashorynejad, H.R. "Investigation of squeezing unsteady nanofluid flow using ADM", *Powder Technol.*, **239**, pp. 259–265 (2013).

19. Sheikholeslami, M., Bandpy, M.G., and Domairry, G. "Free convection of nanofluid filled enclosure using lattice Boltzmann method (LBM)", *Appl. Math. Mech.*, **34**, pp. 833–846 (2013).

20. Ali, M., Shahzad, M., Sultan, F., et al. "Characteristic of heat transfer in flow of cross nanofluid during melting process", *Appl. Nanosci.*, **10**(12), pp. 5201–5210 (2020).

21. Shah, S.Z.H., Ayub, A., Sabir, Z., et al. "Insight into the dynamics of time-dependent cross nanofluid on a melting surface subject to cubic auto catalysis", *Case Stud. Therm. Eng.*, **27**, p. 101227 (2021).

22. Ayub, A., Wahab, H.A., Shah, S.Z., et al. "Interpretation of infinite shear rate viscosity and a non-uniform heat sink/source on a 3D radiative cross nanofluid with buoyancy assisting/opposing flow", *Heat Transf.*, **50**(5), pp. 4192–4232 (2021).

23. Haider, A., Ayub, A., Madassar, N., et al. "Energy transference in time-dependent Cattaneo-Christov double diffusion of second-grade fluid with variable thermal conductivity", *Heat Transf.*, **50**(8), pp. 8224–8242 (2021).

24. Ayub, A., Sabir, Z., Altamirano, G.C., et al. "Characteristics of melting heat transport of blood with time-dependent cross-nanofluid model using Keller-Box and BVP4C method", *Eng. Comput.*, **38**, pp. 3705–3719 (2022). https://doi.org/10.1007/s00366-021-01406-7

25. Haq, R.U., Nadeem, S., Khan, Z.H., et al. "Thermal radiation and slip effects on MHD stagnation point flow of nanofluid over a stretching sheet", *Physica E Low Dimens. Syst. Nanostruct.*, **65**, pp. 17–23 (2015).

26. Ellahi, R. and Riaz, A. "Analytical solutions for MHD flow in a third-grade fluid with variable viscosity", *Math. Comput. Model.*, **52**, pp. 1783–1793 (2010).

27. Ramesh, K. and Sharma, T. "Effectiveness of radiation and Joule heating on hydromagnetic Carreau fluid through microfluidic channels with slip boundary conditions", *Microsyst. Technol.*, **24**, pp. 4921–4932 (2018).

28. Dogonchi, A.S., Alizadeh, M., and Ganji, D.D. "Investigation of MHD Go-water nanofluid flow and heat transfer in a porous channel in the presence of thermal radiation effect", *Adv. Powder Technol.*, **28**, pp. 1815–1825 (2017).

29. Pushpa, B.V., Sankar, M., and Mebarek-Oudina, F. "Buoyant convective flow and heat dissipation of Cu-H_2O nanoliquids in an annulus through a thin baffle", *Journal of Nanofluids*, **10**(2), pp. 292–304 (2021). https://doi.org/10.1166/jon.2021.1782

30. Khan, U., Mebarek-Oudina, F., Zaib, A., et al. "An exact solution of a Casson fluid flow induced by dust particles with hybrid nanofluid over a stretching sheet subject to Lorentz forces", *Waves in Random and Complex Media* (2022). https://doi.org/10.1080/17455030.2022.2102689

31. Kandasamy, R., Mohammad, R., Zailani, N.A.B.M., et al. "Nanoparticle shapes on squeezed MHD nanofluid flow over a porous sensor surface", *J. Mol. Liq.*, **233**, pp. 156–165 (2017).

32. Nadeem, S. and Akbar, N.S. "Effects of heat transfer on the peristaltic transport of MHD Newtonian fluid with variable viscosity: application of Adomian decomposition method", *Commun. Nonlinear Sci. Numer. Simul.*, **14**, pp. 3844–3855 (2009).

33. Nadeem, S. and Akram, S. "Heat transfer in a peristaltic flow of MHD fluid with partial slip", *Commun. Nonlinear Sci. Numer. Simul.*, **15**, pp. 312–321 (2010).

34. Warke, A.S., Ramesh, K., Mebarek-Oudina, F., et al. "Numerical investigation of nonlinear radiation with magneto-micropolar stagnation point flow past a heated stretching sheet", *J. Therm. Anal. Calorim.*, **147**(12), pp. 6901–6912 (2022). https://doi.org/10.1007/s10973-021-10976-z.

35. Srinivas, S. and Kothandapani, M. "The influence of heat and mass transfer on MHD peristaltic flow through a porous space with compliant walls", *Appl. Math. Comput.*, **213**, pp. 197–208 (2009).

36. Hayat, T. and Hina, S. "The influence of wall properties on the MHD peristaltic flow of a Maxwell fluid

with heat and mass transfer", *Nonlinear Anal. Real World Appl.*, **11**, pp. 3155–3169 (2010).

37. Dharmaiah, G., Mebarek-Oudina, F., Sreenivasa Kumar, M., et al. "Nuclear reactor application on Jeffrey fluid flow with Falkner-skan factor, Brownian and thermophoresis, non linear thermal radiation impacts past a wedge", *Journal of the Indian Chemical Society*, **100**(2), 100907 (2023). https://doi.org/10.1016/j.jics.2023.100907

38. Chabani, I., Mebarek-Oudina, F., and Ismail, A.I. "MHD flow of a hybrid nano-fluid in a triangular enclosure with zigzags and an elliptic obstacle", *Micromachines*, **13**(2), p. 224 (2022). https://doi.org/10.3390/mi13020224

39. Shah, S.Z.H., Fathurrochman, I., Ayub, A., et al. "Inclined magnetized and energy transportation aspect of infinite shear rate viscosity model of Carreau nanofluid with multiple features over wedge geometry", *Heat Transfer*, **51**(2), pp. 1622–1648 (2022).

40. Swain, K., Mahanthesh, B., and Mebarek-Oudina, F. "Heat transport and stagnation-point flow of magnetized nanoliquid with variable thermal conductivity with Brownian moment and thermophoresis aspects", *Heat Transfer*, **50**(1), pp. 754–764 (2021). https://doi.org/10.1002/htj.21902

41. Shah, S.Z., Wahab, H.A., Ayub, A., et al. "Higher order chemical process with heat transport of magnetized cross nanofluid over wedge geometry", *Heat Transfer*, **50**(4), pp. 3196–3219 (2021).

42. Mebarek-Oudina, F. and Chabani, I. "Review on Nano-fluids applications and heat transfer enhancement techniques in different enclosures", *Journal of Nanofluids*, **11**(2), pp. 155–168 (2022). https://doi.org/10.1166/jon.2022.1834

43. Asogwa, K., Mebarek-Oudina, F., and Animasaun, I. "Comparative investigation of water-based Al_2O_3 nanoparticles through water-based CuO nanoparticles over an exponentially accelerated radiative Riga plate surface via heat transport", *Arabian Journal for Science and Engineering*, **47**, pp. 8721–8738 (2021). https://doi.org/10.1007/s13369-021-06355-3

44. Marzougui, S., Mebarek-Oudina, F., Mchirgui, A., et al. "Entropy generation and heat transport of Cu-water nanoliquid in porous lid-driven cavity through magnetic field", *International Journal of Numerical Methods for Heat & Fluid Flow*, **32**(6), pp. 2047–2069 (2022). https://doi.org/10.1108/HFF-04-2021-0288

45. Dadheech, P.K., Agrawal, P., Mebarek-Oudina, F., et al. "Comparative heat transfer analysis of $MoS_2/C_2H_6O_2$ and MoS_2-$SiO_2/C_2H_6O_2$ nanofluids with natural convection and inclined magnetic field", *Journal of Nanofluids*, **9**(3), pp. 161–167 (2020). https://doi.org/10.1166/jon.2020.1741

46. Rajashekhar, C., Mebarek-Oudina, F., Vaidya, H., et al. "Mass and heat transport impact on the peristaltic flow of Ree-Eyring liquid with variable properties for hemodynamic flow", *Heat Transfer*, **50**(5), pp. 5106–5122 (2021). https://doi.org/10.1002/htj.22117

47. Hassan, M., Mebarek-Oudina, F., Faisal, A., et al. "Thermal energy and mass transport of shear thinning fluid under effects of low to high shear rate viscosity", *International Journal of Thermofluids*, **15**, p. 100176 (2022). https://doi.org/10.1016/j.ijft.2022.100176

48. Gowda, R.J.P., Kumar, R.N., Aldalbahi, A., et al. "Thermophoretic particle deposition in time dependent flow of hybrid nanofluid over rotating and vertically upward/downward moving disk", *Surf. Interfaces*, **22**, p. 100864 (2021).

49. Ali, R., Asjad, M.I., Aldalbahi, A., et al. "Convective flow of a Maxwell hybrid nanofluid due to pressure gradient in a channel", *J. Therm. Anal. Calorim.*, **143**, pp. 1319–1329 (2021). https://doi.org/10.1007/s10973-020-10304-x

50. Dhif, K., Mebarek-Oudina, F., Chouf, S., et al. "Thermal analysis of the solar collector cum storage system using a hybrid-nanofluids", *Journal of Nanofluids*, **10**(4), pp. 634–644 (2021). https://doi.org/10.1166/jon.2021.1807

51. Djebali, R., Mebarek-Oudina, F., and Choudhari, R. "Similarity solution analysis of dynamic and thermal boundary layers: further formulation along a vertical flat plate", *Physica Scripta*, **96**(8), p. 085206 (2021). https://doi.org/10.1088/1402-4896/abfe31

52. Choudhari, R., Mebarek-Oudina, F., Öztop, H.F., et al. "Electro-osmosis modulated peristaltic flow of non-Newtonian liquid via a microchannel and variable liquid properties", *Indian J. Phys.*, **96**, pp. 3853–3866 (2022). https://doi.org/10.1007/s12648-022-02326-y

53. Sridhar, V. and Ramesh, K. "Peristaltic activity of thermally radiative magneto-nanofluid with electroosmosis and entropy analysis", *Heat Transf.*, **51**(2), pp. 1668–1690 (2022).

54. Munawar, S. and Saleem, N. "Entropy generation in thermally radiated hybrid nanofluid through an electroosmotic pump with ohmic heating: Case of synthetic cilia regulated stream", *Sci. Prog.*, **104**(3), pp. 1–22 (2021).

55. Ijaz, N., Zeeshan, A., and Rehman, S.U. "Effect of electro-osmosis and mixed convection on nano-biofluid with non-spherical particles in a curved channel", *Mech. Ind.*, **19**(1), p. 108 (2018).

56. Mandal, S., Ghosh, U., Bandopadhyay, A., et al. "Electro-osmosis of superimposed fluids in the presence of modulated charged surfaces in narrow confinements", *J. Fluid Mech.*, **776**, pp. 390–429 (2015).

57. Ghorbani, S., Moghadam, A.J., Emamian, A., et al. "Numerical simulation of the electroosmotic flow of the Carreau-Yasuda model in the rectangular microchannel", *Int. J. Numer. Methods Heat Fluid Flow.*, **32**(7), pp. 2240–2259 (2021). https://doi.org/10.1108/HFF-07-2021-0495.

58. Murtaza, S., Iftekhar, M., Ali, F., et al. "Exact analysis of non-linear electro-osmotic flow of generalized Maxwell nanofluid: applications in concrete based nano-materials", *IEEE Access*, **8**, pp. 96738–96747 (2020).

59. Noreen, S., Waheed, S., and Hussanan, A. "Peristaltic motion of MHD nanofluid in an asymmetric microchannel with Joule heating, wall flexibility and different zeta potential", *Bound. Value Probl.*, **2019**(1), pp. 1–23 (2019).
60. Mahapatra, B. and Bandopadhyay, A. "Numerical analysis of combined electroosmotic-pressure driven flow of a viscoelastic fluid over high zeta potential modulated surfaces", *Phys. Fluids*, **33**(1), p. 012001 (2021).
61. Ramesh, K. and Prakash, J. "Thermal analysis for heat transfer enhancement in electroosmosis-modulated peristaltic transport of Sutter by nanofluids in a microfluidic vessel", *J. Therm. Anal. Calorim.*, **138**(2), pp. 1311–1326 (2019).

Biographies

Katta Ramesh is working as a Senior Lecturer at the School of Mathematical Sciences, Sunway University, Malaysia. He received his PhD in Applied Mathematics (Modelling of physiological flows) in 2016 from Visvesvaraya National Institute of Technology, India. He has published more than 65 papers in reputed international journals, 2 book chapters, and 2 conference proceedings. He has achieved world rank 855 and Indian rank 34 in top 2% scientists across the world as per updated science-wide author database of standardized citation indicators in the field of Mechanical Engineering and Transport published in 2021. His research work attempts at the mathematical modelling and simulation of biological flows of biofluids/nanofluids/hybrid nanofluids/ternary nanofluids, microfluidics, computational fluid dynamics, and heat and mass transfer.

Fateh Mebarek Oudina received PhD in 2010 and published more than 140 papers in reputed international journals and proceeding. Currently, he works at Skikda University in Algeria and serves as a reviewer for more than 250 indexed international journals. His name was included in all American Stanford University lists "Top 2% Best Scientists in the World". Email address: oudina2003@yahoo.fr / f.mebarek_oudina@univ-skikda.dz ORCID ID: 0000-0001-6145-8195

Abdel Aziz I. Ismail received PhD in 1994 from Stuttgart University. He has published more than 80 papers in reputed international journals and proceeding. Currently, he works at Umm Al-Qura University in Saudi Arabia and serves as a reviewer for more than 150 indexed international journals. He worked at TANTA University, EGYPT.

Bharat Raj Jaiswal is working as an Assistant Professor at the Symbiosis Institute of Technology, India. He earned his PhD in Applied Mathematics (Stokes flow over axisymmetric bodies) in 2015 from Jaypee University of Engineering and Technology, India. He has over 20 research papers published in prestigious international journals as well as 2 conference proceedings. He has given expert lectures and been invited to speak at conferences. He is a life-time member of various professional bodies such as Indian Science Congress Association, Indian Society of Theoretical and Applied Mechanics, Indian Mathematical Society, and Ramanujan Mathematical Society. His research interests include Stokes flow analysis, flow through porous media, and multiphase flow.

Arundhati Suresh Warke received her PhD from University of Pune and is a Professor in Mathematics, Symbiosis Institute of Technology, Pune, India. She has 39 years of teaching and 21 years of research experience, and the research interest areas are mathematical modeling of fluid flow, blood flow, non-linear waves, and modeling of heat and mass transfer. She has more than 60 papers published in journals of high repute, and 3 book chapters have been published in books published by Springer. She has delivered lectures in international conferences and other engineering institutes.

Ram Kishun Lodhi is an Assistant Professor at the Department of Applied Science, Symbiosis Institute of Technology, India. He received his PhD from Jaypee University of Engineering & Technology, India in 2017. He is a reviewer of several journals. He has published 14 research papers in well-reputed journals. His current research mainly covers singular perturbation problems, spline methods, and analytical and numerical solutions of linear and nonlinear problems.

Tushar Sharma received his MSc degree from Lovely Professional University, India. Currently, he is working as a subject matter expert at Chegg private limited. He has published one research article in a well-reputed journal.